Robust Effective Ground State in a Nonintegrable Floquet Quantum Circuit

Tatsuhiko N. Ikeda,[1,2] Sho Sugiura,[3,4,5] and Anatoli Polkovnikov[2]
[1]RIKEN Center for Quantum Computing, Wako, Saitama 351-0198, Japan
[2]Department of Physics, Boston University, Boston, Massachusetts 02215, USA
[3]Blocq, Inc., Toranomon Hills Business Tower 1-17-1 Toranomon, Minato, Tokyo 105-6416 Japan
[4]Physics and Informatics Laboratory, NTT Research, Inc., Sunnyvale, California 94085, USA
[5]Laboratory for Nuclear Science, Massachusetts Institute of Technology, Cambridge, Massachusetts 02139, USA

(Received 5 December 2023; revised 21 May 2024; accepted 5 June 2024; published 17 July 2024)

An external periodic (Floquet) drive is believed to bring any initial state to the featureless infinite temperature state in generic nonintegrable isolated quantum many-body systems in the thermodynamic limit, irrespective of the driving frequency Ω. However, numerical or analytical evidence either proving or disproving this hypothesis is very limited and the issue has remained unsettled. Here, we study the initial state dependence of Floquet heating in a nonintegrable kicked Ising chain of length up to $L = 30$ with an efficient quantum circuit simulator, showing a possible counterexample: the ground state of the effective Floquet Hamiltonian is exceptionally robust against heating, and could stay at finite energy density even after infinitely many Floquet cycles, if the driving period is shorter than a threshold value. This sharp energy localization transition or crossover does not happen for generic excited states. The exceptional robustness of the ground state is interpreted by (i) its isolation in the energy spectrum and (ii) the fact that those states with L-independent $\hbar\Omega$ energy above the ground state energy of any generic local Hamiltonian, like the approximate Floquet Hamiltonian, are atypical and viewed as a collection of noninteracting quasiparticles. Our finding paves the way for engineering Floquet protocols with finite driving periods realizing long-lived, or possibly even perpetual, Floquet phases by initial state design.

DOI: 10.1103/PhysRevLett.133.030401

Introduction.—Periodically driven, or Floquet, quantum systems have recently attracted renewed attention from the viewpoint of Floquet engineering, i.e., creating intriguing functionalities of matter with external periodic drives [1–5], together with rapid developments of experimental techniques, such as strong light-matter interactions and driven artificial quantum matter [6–10]. In isolated systems Floquet-engineered states are believed to break down eventually due to heating [11–13], i.e., the energy injection accompanied by the drive, and stability of Floquet engineering has been a central issue. For general local Hamiltonians with bounded local energy spectrum, rigorous upper bounds on heating are known and guarantee that the heating is suppressed exponentially in the driving frequency Ω irrespective of the initial states [14–16]. Many experimental [17–20] and numerical [21–30] studies observe actual heating rates obeying the exponential scaling consistent with these bounds in generic Hamiltonians with some notable exceptions [31–38]. At the same time it is known that these bounds cannot be tight. For example, exponential heating was also observed in classical systems, where these bounds diverge due to the infinite local Hilbert-space size [39,40].

At the same time, some numerical studies report indications of very sharp phase transitionlike behavior of heating when the driving frequency is varied [32,41–45]. Namely, below (above) a threshold frequency, the system remains at a finite (is brought to the infinite) temperature after many driving cycles. This sharp transition has also been translated to Trotterization on digital quantum computers, and the longtime Trotter error, a counterpart of heating, has been discussed [35,43,44]. Yet those results cannot be conclusively extrapolated to the thermodynamic limit because of potentially large finite-size effects. In a one-body chaotic model [43] and a special integrable model [45], such a Trotter transition has been analytically obtained. On the other hand, some studies report smooth crossovers rather than a transition in generic nonintegrable models [12]. Those studies differ in many ways, including the model, initial states, physical observables, etc., and it has yet to be understood whether and in what sense a phase transition exists in generic nonintegrable many-body models.

In this Letter, we show numerical evidence for the Trotter (or heating) transition in a nonintegrable kicked Ising model by reaching as large as $L = 30$ spins with an efficient

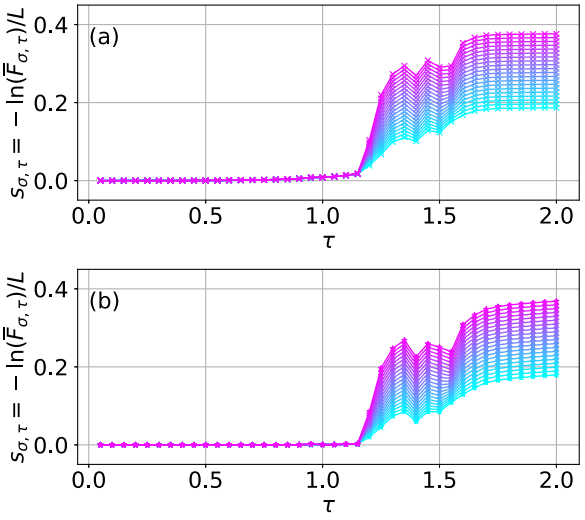

FIG. 1. Time-averaged fidelity (5) in the log scale under the Floquet evolution (1) starting from the ground states of (a) $H_F^{(0)}$ and (b) $H_F^{(2)}$. The system size is $L = 24$, and plot colors from light blue to magenta correspond to the time cutoff σ from 10^2 to 10^4 equidistant in the log scale.

quantum circuit simulator (see Fig. 1). The sharp transition is absent for most initial states but is most conspicuously seen when the initial state is the effective ground state (GS), i.e., the ground state of an effective Hamiltonian in the high-frequency expansion. It becomes sharper and sharper if we increase the order of the expansion, but the transition point is insensitive to this order. We interpret the exceptional robustness of the effective ground state by the generic property of local Hamiltonians that the energetically resonant states with the ground state above energy $\hbar\Omega = O(1)$ consist of a few quasiparticles behaving freely in the thermodynamic limit. The initial state dependence of the transition sheds new light on the seemingly contradicting previous reports about the presence or absence of transitions. Besides, the stability of states above a critical drive frequency (i.e., below a critical Trotter step) encourages Floquet engineering (Trotter simulations) for a long time even in the thermodynamic limit without the need of scaling the Trotter step down to zero with increasing the simulation time [35].

Formulation of the problem.—We consider a quantum spin-1/2 chain of length L under the following time-periodic Hamiltonian

$$H(t) = \begin{cases} H_1 & \left(k \le t/\tau < k + \frac{1}{2}\right), \\ H_2 & \left(k + \frac{1}{2} \le t/\tau < k + \frac{3}{2}\right), \\ H_1 & \left(k + \frac{3}{2} \le t/\tau < k + 2\right), \end{cases} \tag{1}$$

where $k \in \mathbb{Z}$ and 2τ is the driving period, and

$$H_1 = -\sum_{j=1}^{L}\left(\frac{J}{4}\sigma_j^z\sigma_{j+1}^z + \frac{h}{2}\sigma_j^z\right), \qquad H_2 = -\frac{g}{2}\sum_{j=1}^{L}\sigma_j^x. \tag{2}$$

Here, σ_j^x and σ_j^z are the Pauli matrices acting on the site j, and the periodic boundary conditions are imposed while Ref. [35] used the open ones. Throughout this Letter, we set $J = h = g = 1$ since we have confirmed that the results are not sensitive to their choice as long as they are far away from integrable points. An initial state $|\psi_{\rm ini}\rangle$ unitarily evolves in time under $H(t)$, and the state at $t = n\tau (n \in \mathbb{Z})$ is given by $|\psi(2n\tau)\rangle = T(\tau)^n|\psi_{\rm ini}\rangle$ with

$$T(\tau) = e^{-iH_1\frac{\tau}{2}}e^{-iH_2\tau}e^{-iH_1\frac{\tau}{2}}. \tag{3}$$

We ask now how stable $|\psi(2n\tau)\rangle$ is under the periodic drive. To quantify the stability, we introduce the following fidelity [46]:

$$F(n,\tau) = |\langle\psi_{\rm ini}|T(\tau)^n|\psi_{\rm ini}\rangle|^2. \tag{4}$$

This definition is motivated by the following reasoning. The Magnus expansion (or the symmetric Baker-Campbell-Hausdorff formula) gives us a power series expansion for H_F defined through $T(\tau) = e^{-iH_F\tau}$ as $H_F = \sum_{l=0}^{\infty} h^{(2l)}\tau^{2l}$, where odd-order terms all vanish due to the symmetry $T(-\tau) = T^\dagger(\tau)$. Then a truncated effective Hamiltonian $H_F^{(2k)} = \sum_{l=0}^{k} h^{(2l)}\tau^{2l}$ gives an approximation $U_{2k}(\tau) = e^{-iH_F^{(2k)}\tau} = T(\tau) + O(\tau^{2k+3})$. The approximate unitary $U_{2k}(\tau)$ is generated by the time-independent Hamiltonian $H_F^{(2k)}$ and thus energy conserving, and the time evolution $|\psi_{2k}(2n\tau)\rangle = U_{2k}(n\tau)|\psi_{\rm ini}\rangle$ is free from Floquet heating. If $|\psi_{\rm ini}\rangle$ is an eigenstate of $H_F^{(2k)}$ (as we will assume below), the fidelity between the exact and approximate states $|\langle\psi_{2k}(2n\tau)|\psi(2n\tau)\rangle|^2$ [43,44] reduces to Eq. (4). While Ref. [46] showed that eigenstates are more stable than the superposition of them, we address which of the eigenstates are more stable. We note that the above argument is also translated to Trotterization; $T(\tau)$ is a $(2k+2)$th order Trotter approximation for $U_{2k}(n\tau)$ generated by the target Hamiltonian $H_F^{(2k)}$. To focus on the longtime stability, we introduce the long- but finite-time average of the fidelity:

$$\bar{F}_{\sigma,\tau} = \frac{1}{\mathcal{N}_\sigma}\sum_{n=0}^{\infty}F(n,\tau)e^{-(n/\sigma)^2}, \tag{5}$$

where $\mathcal{N}_\sigma := \sum_{n=0}^{\infty} e^{-(n/\sigma)^2}$ and $\sigma(>0)$ denotes a Gaussian cutoff. The time-averaged fidelity is numerically obtained by calculating $T(\tau)^n|\psi_{\rm ini}\rangle$ for $n = 0, 1, \ldots, n_{\max}$ so that $n_{\max} \gg \sigma$. Since $T(\tau)$ can be represented by 1- and 2-qubit quantum gates unlike other Floquet models [12], $T(\tau)^n|\psi_{\rm ini}\rangle$ is more efficiently calculated using a circuit simulator [47].

Sharp Trotter transition for the Floquet ground state.—Figure 1 shows the τ dependence of the time-averaged fidelity when the initial state is what we call here the

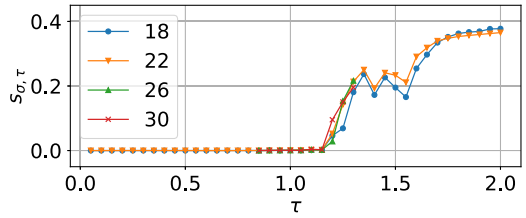

FIG. 2. System-size dependence of time-averaged fidelity (5). Here, the initial state is the ground state of $H_F^{(2)}$ and the cutoff is $\sigma = 5 \times 10^3$.

effective Floquet ground state, i.e., the ground state of $H_F^{(0)} = H_1 + H_2$ and $H_F^{(2)}$. We remark that the Floquet ground state is not an eigenstate of $T(\tau)$ and hence $F(n, \tau)$ evolves in n. For convenience, we plot the rate function

$$s_{\sigma,\tau} = -L^{-1} \ln(\bar{F}_{\sigma,\tau}), \tag{6}$$

which is expected to have a well-defined thermodynamic limit assuming the typical system size scaling $\bar{F}_{\sigma,\tau} = e^{-s_{\sigma,\tau} L}$ and a larger (smaller) $s_{\sigma,\tau}$ corresponding to a smaller (larger) fidelity. If the unitary $T(\tau)$ can be represented as $T(\tau) = e^{-iH_F \tau}$ with H_F being a local gapped Hamiltonian then, $s_{\sigma,\tau}$ is expected to be a small number well defined in the joint limit $\sigma \to \infty$, $L \to \infty$. As Fig. 1(a) shows, for $\tau < 1.2$, $s_{\sigma,\tau}$ smoothly depends on τ and is almost independent of σ, whereas it increases abruptly in $\tau \geq 1.2$ and simultaneously acquires strong σ dependence. Thus the GS of $H_F^{(0)}$ is, at least, strongly robust against heating for $\tau < 1.2$. This transitionlike behavior at $\tau \approx 1.2$ becomes more conspicuous when the initial state is the ground state of $H_F^{(2)}$, for which the fidelity remains almost constant all the way to the transition point $\tau = 1.2$. Note that this behavior is similar to what was obtained in an integrable circuit [45] for a special initial state, whereas our circuit is nonintegrable.

It is noteworthy that the threshold value $\tau \approx 1.2$ does not correspond to the known convergence radius of the Magnus expansion. Although some radii are known, each dictates that the expansion is convergent if $(\|H_1\| + \|H_2\|)\tau < r$, where $\|\cdots\|$ denotes the 2-norm, and r is a constant, e.g., $r = \pi$ [48]. Considering that both $\|H_1\|$ and $\|H_2\|$ are $O(L)$, we learn that those convergence radii are $O(L^{-1})$ and shrink as L increases. On the contrary, the transitionlike behavior of the fidelity is robust for larger systems. Figure 2 compares the fidelities at different system sizes at a fixed time cutoff $\sigma = 5 \times 10^3$. In the small-τ regime $\tau < 1.2$, we observe little dependence on L, suggesting the stability of the Floquet ground state in the thermodynamic limit. We note that $s_{\sigma,\tau}$ shows a small bump at $\tau = 1.1$, visible on the log scale. This bump likely reflects an accidental many-body resonance [49]. We observe that it weakens with increasing system size such that our numerical results are consistent with the scenario that it vanishes in the thermodynamic limit $L \to \infty$.

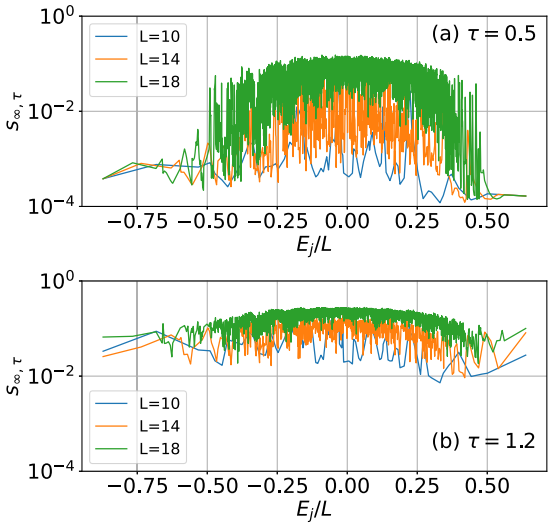

FIG. 3. Scaled long-time fidelity error (6) for each eigenstate $|\psi_{\text{ini}}\rangle = |E_j\rangle$ calculated by Eq. (9). The Trotter steps are (a) $\tau = 0.5$ and (b) 1.2. Each color distinguishes the system sizes as in the legends.

Before looking into the interplay of the system size and the time cutoff, we examine other eigenstates of $H_F^{(2k)}$ chosen for the initial state. For computational convenience, we calculate the infinite-time average $\bar{F}_{\infty,\tau}$ for each eigenstate $|E_j\rangle$ of $H_F^{(0)}$, i.e.,

$$H_F^{(0)}|E_j\rangle = E_j|E_j\rangle \tag{7}$$

for $j = 0, \ldots, d-1$. Considering the translation and inversion symmetries shared by $T(\tau)$ and $H_F^{(0)}$, we restrict ourselves to the symmetry sector of the zero momentum and the even parity that hosts the ground state, and d denotes the dimension of this symmetry sector. Using the eigenstates of $T(\tau)$,

$$T(\tau)|\theta_\alpha\rangle = e^{-i\theta_\alpha}|\theta_\alpha\rangle \tag{8}$$

and assuming there is no degeneracy in the eigenvalues, we obtain

$$\bar{F}_{\infty,\tau} = \sum_\alpha |\langle\theta_\alpha|E_j\rangle|^4; \qquad s_{\infty,\tau} = -L^{-1} \ln(\bar{F}_{\infty,\tau}). \tag{9}$$

Figure 3 shows $s_{\infty,\tau}$ for all $|\psi_{\text{ini}}\rangle = |E_j\rangle$ $(j = 0, \ldots, d-1)$. The panel (a) is for $\tau = 0.5$ below the crossover, where we observe that the GS $(j = 0)$, as well as the highest-excited state (HES, $j = d-1$), are consistent with the behavior $s_{\infty,\tau} = \text{const}(L) \ll 1$. Note that this stability holds after the infinite Floquet cycles, without finite cutoff σ, at least up to $L \leq 18$. In contrast, $s_{\infty,\tau}$ tends to increase in the middle

of the spectrum as L increases, meaning the faster than exponential decay of fidelity with the system size. For $\tau = 1.2$ in the crossover, on the other hand, $s_{\infty,\tau}$ increases with L for all states, including the GS and HES. These results highlight the uniqueness of the GS and HES and potentially a few more nearby states as compared to other eigenstates. Namely the sharp crossover in fidelity (and other heating measures) seen for the GS in Fig. 1 is not present for generic initial eigenstates of $H_F^{(2k)}$. This finding seems rather unexpected as, naively, the notion of the ground state is not well defined for the Floquet unitary.

A physical interpretation for the unexpected robustness of the GS (and HES) is based on the breakdown of Fermi's golden rule (FGR) description of Floquet heating [58,59] as microscopic transitions among a continuum of eigenstates [49]. First, we note that our unitary evolution (3) is a special case of general Floquet evolution generated by a time-periodic Hamiltonian $H(t) = H_0 + \epsilon g(t) K$. In fact, Eq. (3) realizes when $H_0 = (H_1 + H_2)/2$, $g(t) = \mathrm{sgn}[\cos(\Omega t)]$ with $\Omega = \pi/\tau$, $K = (H_0 - H_1)/2$, and $\epsilon = 1$. At small driving amplitudes ϵ, the matrix elements $|\langle E_{j'}|K|E_0\rangle|^2$ excite the ground state into excited states at resonance $E_{j'} \approx E_0 + \Omega$. Importantly, we are considering L-independent Ω, and, in a standard scenario of local models, such lowest excitations $|E_{j'}\rangle$ can be viewed as a subextensive number of noninteracting quasiparticles with infinite lifetimes [60]. In other words generic quantum systems at low energies behave as if they are free. As the system size increases this picture becomes more and more accurate. However, the noninteracting systems with bounded quasiparticle spectrum cannot absorb energy beyond their single or two-particle bandwidth. This, for example, follows from exponential, not factorial, operator spreading in the Krylov space [16]. This suppression of heating does not work for most excited states, i.e., if the initial energy E_j is $O(L)$ above the ground energy, because it transitions into $E_{j'}$ with $E_{j'} \approx E_j + \Omega$ and these are dense and do not have quasiparticle description. Interestingly, our analysis shows that this picture remains qualitatively unchanged if the driving amplitude ϵ is not small and the matrix elements of the unitary $\delta U = U_{2k}^\dagger(\tau) T(\tau)$ replace the matrix elements of K in the FGR analysis [30]. This robustness of the FGR threshold follows from the fact that within one driving period, the operators do not have time to spread, and hence δU remains a quasilocal operator at any ϵ.

Approximate quantum many-body scars.—Now we return to the numerical analysis of the properties of the Floquet GS. Equation (9) dictates that the time-averaged fidelity is governed by the overlap between the initial state and the Floquet eigenstates. Thus, the robustness of the Floquet ground state suggests the presence of a special eigenstate of the unitary $T(\tau)$, which is similar to the ground state of a local static Hamiltonian. We visualize the

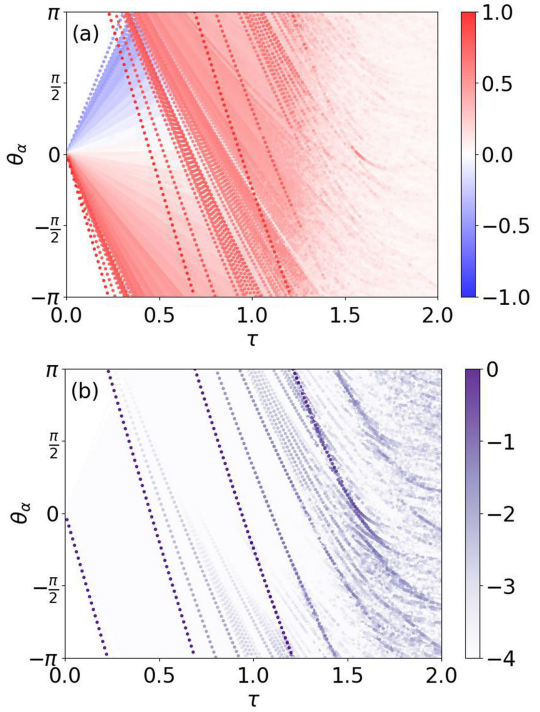

FIG. 4. All the θ_α's plotted for various τ at system size $L = 16$. The color of each data point shows (a) the magnetization expectation value $\langle\theta_\alpha|m_z|\theta_\alpha\rangle$ and (b) the overlap with $H_F^{(0)}$'s GS, $\log_{10}|\langle E_0|\theta_\alpha\rangle|^2$. In panel (b), all the values less than -4 correspond to white color.

Floquet eigenstates $|\theta_\alpha\rangle$ in Fig. 4(a), where we plot all the eigenvalues θ_α for various τ. These eigenvalues are color coded according to their average magnetization $\langle\theta_\alpha|m_z|\theta_\alpha\rangle$ with $m_z = L^{-1}\sum_{i=1}^L Z_i$.

A perturbation theory from $\tau = 0$ allows us to interpret Fig. 4(a) for small τ. Namely, we regard $U_0 = e^{-iH_F^{(0)}\tau}$ as the unperturbed operator and $V \coloneqq T(\tau) - e^{-iH_F^{(0)}\tau} = O(\tau^3)$ as the perturbation. The eigenstates of $H_F^{(0)}$ defined in Eq. (7) satisfy $U_0|E_j\rangle = e^{-iE_j\tau}$, meaning $|\theta_j\rangle \approx |E_j\rangle$ with $\theta_j \equiv E_j\tau (\mathrm{mod}\, 2\pi)$ at the zeroth order. If τ is so small that $|E_j|\tau < \pi$ holds for every j, the modulo can be ignored, and the relations $\theta_j = E_j\tau (j = 0, 1, \ldots, d-1)$ are seen in Fig. 4(a) for $\tau \lesssim 0.2$. Here, the lowest (highest) branch of data is connected to the GS (HES) of $H_F^{(0)}$ in $\tau \to 0^+$.

Once some of $|E_j|\tau$ exceeds π as τ increases, the eigenvalues θ_α are folded into the interval $[-\pi, \pi)$, which start to happen at $\tau \gtrsim 0.3$ [see Fig. 4(a)]. The first folding occurs when $\|H_F^{(0)}\|\tau = \pi$, i.e., $\tau = O(L^{-1})$, which scales with L like the convergence radius of the Magnus expansion. After the folding, there appear pairs of eigenvalues of $U_0(\tau)$: $(e^{-iE_{j_1}\tau}, e^{-iE_{j_2}\tau})$ coming closer, around which the perturbation V is expected to hybridize the corresponding eigenstates. Such hybridization should manifest as repulsion of magnitude $\sim|\langle E_{j_1}|V|E_{j_2}\rangle|$ between them.

Nevertheless, the ground-state and a few low-energy-state branches are robust even after the folding occurs, and the eigenvalues come across numerous other eigenvalues up to $\tau \approx 1.2$. Strictly speaking, there are level repulsions (see Supplemental Material [49]), but these are very small and difficult to observe without fine-tuning τ (see also discussions below). This is consistent with the expectation that the off-diagonal elements $\langle E_{j_1}|V|E_{j_2}\rangle$ are exponentially small in $|E_{j_1} - E_{j_2}|$, according to the off-diagonal eigenstate thermalization hypothesis [61,62]. We regard the robust eigenstates in the middle of the spectrum as the approximate many-body scar states since they are weakly mixed with the other states without any symmetry protection. Similar robustness also exists near the HES branch, which becomes visible in reverse magnetization color-code plotting [49].

The important role of the robust branches of Floquet eigenstates is shown in Fig. 4(b), which is a similar plot with the color being replaced by the overlap with the effective Floquet ground state, $|\langle E_0|\theta_\alpha\rangle|^2$ (in the log scale). As the figure shows, only the ground-state branch is significantly populated for $\tau \lesssim 0.5$, a few other branches become gradually populated for $0.5 \lesssim \tau \lesssim 1.2$, and the population scatters between states finally for $\tau \gtrsim 1.2$. These behaviors correspond to the smooth decrease of the fidelity (i.e., the increase of $s_{\sigma,\tau}$) in Fig. 1(a) up to $\tau < 1.2$ and its abrupt change in $\tau > 1.2$. A similar argument also holds when $|E_0\rangle$ is replaced by the GS of $H_F^{(2)}$, for which the overlap is concentrated even more on the GS branch.

Role of the time cutoff σ.—Finally, we turn to $\sigma < \infty$ and discuss its role in removing spiky behaviors in $\bar{F}_{\infty,\tau}$ due to tiny level repulsions. Note that

$$\bar{F}_{\sigma,\tau} = \sum_\alpha |c_\alpha|^4 + 2\sum_{\alpha<\beta} |c_\alpha|^2 |c_\beta|^2 D_\sigma(\theta_\alpha - \theta_\beta), \qquad (10)$$

where $c_\alpha = \langle\theta_\alpha|\psi_{\rm ini}\rangle$ and $D_\sigma(x) = (2\mathcal{N}_\sigma)^{-1} \times (1 + \sum_{n=-\infty}^{\infty} e^{-(n/\sigma)^2 + inx})$, and $D_\sigma(x)$ has narrow peaks at $x = 2\pi\mathbb{Z}$ of width $\sim\sigma^{-1}$ [49]. If we take the limit $\sigma \to \infty$ first with $L < \infty$ fixed, the second term in Eq. (10) vanishes and this equation reduces to Eq. (9). As this expression changes significantly at each level repulsion, $\bar{F}_{\infty,\tau}$ becomes spiky.

The opposite order of limits, i.e., $L \to \infty$ first and $\sigma \to \infty$ second, would avoid the issue originating from the level repulsions, allowing one to study the thermodynamic limit for the shorter periods $\tau \lesssim 1.2$. This is because the second term in Eq. (10) can eliminate the spiky behavior of the first term if σ^{-1} is larger than the tiny resonant level splittings, which exponentially go down with L [49]. The numerical results are consistent with the scenario that if we take this order of limits then we can still observe a very sharp crossover as shown in Figs. 1 and 2, while at the same time eliminating the contribution of the accidental resonant spikes.

Conclusions and outlook.—We have shown strong evidence for a very sharp crossover or possibly even a phase transition in the longtime stability under a Floquet drive or Trotterized dynamics. This transition has been well characterized using the effective Floquet ground state and taking the appropriate order of limits: $L \to \infty$ and then $\sigma \to \infty$. Despite the common belief that all states eventually heat up to the infinite temperature under generic nonintegrable Floquet models, our results suggest that there are exceptional states with anomalously low or possibly zero Floquet heating above a critical driving frequency even in the thermodynamic limit. Such states can be very interesting from the point of view of Floquet engineering because they are extremely long-lived. We interpret the exceptional robustness of the Floquet ground state as a result of emergent free quasiparticle description of the low-energy states of local Hamiltonians with nonextensive energy Ω. Such free quasiparticle systems with a bounded spectrum cannot absorb energy at driving frequencies above few-particle bandwidth.

There remain several open questions. In particular, what is the class of Floquet models where such states exist and how does the number of such stable states scale with the system size [63]? Can we find these states in the classical Floquet systems in the thermodynamic limit? Do such stable states exist for other, non-Floquet, driving protocols? In the extended-space picture [64], where the Floquet drive is represented by coupling to a static photon mode, the Floquet ground states can be viewed as stable midenergy states, as they appear in the middle of the spectrum of the extended static Hamiltonian. As such, they appear to be similar to stable midenergy states discovered in certain static models [65–67]. It remains open to establish a precise correspondence with these models. Of course, it would be very interesting to see such stable states in experimental systems, such as nitrogen-vacancy centers in diamonds and ultracold atoms or ions. This transition as a function of the Trotter step size could also be observed in digital quantum simulators.

Fruitful discussions with Souvik Bandyopadhyay, Marin Bukov, Pieter Claeys, Isaac L. Chuang, Ceren B. Dag, Iliya Esin, Michael Flynn, Asmi Haldar, Martin Holthaus, Pavel Krapivsky, Takashi Oka, Tibor Rakovszky, and Dries Sels are gratefully acknowledged. Numerical exact diagonalization in this work has been performed with the help of the QuSpin package [68,69], and quantum time evolution with Qulacs [47]. T. N. I. was supported by Japan Science and Technology Agency PRESTO Grant No. JPMJPR2112 and by JSPS KAKENHI Grant No. JP21K13852. A. P. was supported by NSF Grant No. DMR- 2103658 and the AFOSR Grant No. FA9550-21-1-0342.

[1] N. Goldman and J. Dalibard, Periodically driven quantum systems: Effective Hamiltonians and engineered gauge fields, Phys. Rev. X **4**, 031027 (2014).

[2] M. Bukov, L. D'Alessio, and A. Polkovnikov, Universal high-frequency behavior of periodically driven systems: From dynamical stabilization to Floquet engineering, Adv. Phys. **64**, 139 (2015).

[3] M. Holthaus, Floquet engineering with quasienergy bands of periodically driven optical lattices, J. Phys. B **49**, 13001 (2015).

[4] A. Eckardt, Colloquium: Atomic quantum gases in periodically driven optical lattices, Rev. Mod. Phys. **89**, 011004 (2017).

[5] T. Oka and S. Kitamura, Floquet engineering of quantum materials, Annu. Rev. Condens. Matter Phys. **10**, 387 (2019).

[6] Y. H. Wang, H. Steinberg, P. Jarillo-Herrero, and N. Gedik, Observation of Floquet-Bloch states on the surface of a topological insulator, Science **342**, 453 (2013).

[7] M. C. Rechtsman, J. M. Zeuner, Y. Plotnik, Y. Lumer, D. Podolsky, F. Dreisow, S. Nolte, M. Segev, and A. Szameit, Photonic Floquet topological insulators, Nature (London) **496**, 196 (2013).

[8] G. Jotzu, M. Messer, R. Desbuquois, M. Lebrat, T. Uehlinger, D. Greif, and T. Esslinger, Experimental realization of the topological Haldane model with ultracold fermions, Nature (London) **515**, 237 (2014).

[9] S. Choi, J. Choi, R. Landig, G. Kucsko, H. Zhou, J. Isoya, F. Jelezko, S. Onoda, H. Sumiya, V. Khemani, C. Von Keyserlingk, N. Y. Yao, E. Demler, and M. D. Lukin, Observation of discrete time-crystalline order in a disordered dipolar many-body system, Nature (London) **543**, 221 (2017).

[10] J. Zhang, P. W. Hess, A. Kyprianidis, P. Becker, A. Lee, J. Smith, G. Pagano, I. D. Potirniche, A. C. Potter, A. Vishwanath, N. Y. Yao, and C. Monroe, Observation of a discrete time crystal, Nature (London) **543**, 217 (2017).

[11] A. Lazarides, A. Das, and R. Moessner, Equilibrium states of generic quantum systems subject to periodic driving, Phys. Rev. E **90**, 012110 (2014).

[12] L. D'Alessio and M. Rigol, Long-time behavior of isolated periodically driven interacting lattice systems, Phys. Rev. X **4**, 041048 (2014).

[13] H. Kim, T. N. Ikeda, and D. A. Huse, Testing whether all eigenstates obey the eigenstate thermalization hypothesis, Phys. Rev. E **90**, 052105 (2014).

[14] T. Kuwahara, T. Mori, and K. Saito, Floquet-Magnus theory and generic transient dynamics in periodically driven many-body quantum systems, Ann. Phys. (Amsterdam) **367**, 96 (2016).

[15] D. A. Abanin, W. De Roeck, W. W. Ho, and F. Huveneers, Effective Hamiltonians, prethermalization, and slow energy absorption in periodically driven many-body systems, Phys. Rev. B **95**, 014112 (2017).

[16] A. Avdoshkin and A. Dymarsky, Euclidean operator growth and quantum chaos, Phys. Rev. Res. **2**, 043234 (2020).

[17] A. Rubio-Abadal, M. Ippoliti, S. Hollerith, D. Wei, J. Rui, S. L. Sondhi, V. Khemani, C. Gross, and I. Bloch, Floquet prethermalization in a Bose-Hubbard system, Phys. Rev. X **10**, 021044 (2020).

[18] K. Viebahn, J. Minguzzi, K. Sandholzer, A.-S. Walter, M. Sajnani, F. Görg, and T. Esslinger, Suppressing dissipation in a Floquet-Hubbard system, Phys. Rev. X **11**, 011057 (2021).

[19] P. Peng, C. Yin, X. Huang, C. Ramanathan, and P. Cappellaro, Floquet prethermalization in dipolar spin chains, Nat. Phys. **17**, 444 (2021).

[20] W. Beatrez, O. Janes, A. Akkiraju, A. Pillai, A. Oddo, P. Reshetikhin, E. Druga, M. McAllister, M. Elo, B. Gilbert, D. Suter, and A. Ajoy, Floquet prethermalization with lifetime exceeding 90 s in a bulk hyperpolarized solid, Phys. Rev. Lett. **127**, 170603 (2021).

[21] M. Bukov, M. Heyl, D. A. Huse, and A. Polkovnikov, Heating and many-body resonances in a periodically driven two-band system, Phys. Rev. B **93**, 155132 (2016).

[22] F. Machado, G. D. Kahanamoku-Meyer, D. V. Else, C. Nayak, and N. Y. Yao, Exponentially slow heating in short and long-range interacting Floquet systems, Phys. Rev. Res. **1**, 033202 (2019).

[23] F. Machado, D. V. Else, G. D. Kahanamoku-Meyer, C. Nayak, and N. Y. Yao, Long-range prethermal phases of nonequilibrium matter, Phys. Rev. X **10**, 011043 (2020).

[24] D. J. Luitz, R. Moessner, S. Sondhi, and V. Khemani, Prethermalization without temperature, Phys. Rev. X **10**, 021046 (2020).

[25] A. Pizzi, D. Malz, G. De Tomasi, J. Knolle, and A. Nunnenkamp, Time crystallinity and finite-size effects in clean Floquet systems, Phys. Rev. B **102**, 214207 (2020).

[26] B. Ye, F. Machado, C. D. White, R. S. Mong, and N. Y. Yao, Emergent hydrodynamics in nonequilibrium quantum systems, Phys. Rev. Lett. **125**, 030601 (2020).

[27] C. Yin, P. Peng, X. Huang, C. Ramanathan, and P. Cappellaro, Prethermal quasiconserved observables in Floquet quantum systems, Phys. Rev. B **103**, 054305 (2021).

[28] C. Fleckenstein and M. Bukov, Prethermalization and thermalization in periodically driven many-body systems away from the high-frequency limit, Phys. Rev. B **103**, L140302 (2021).

[29] C. Fleckenstein and M. Bukov, Thermalization and prethermalization in periodically kicked quantum spin chains, Phys. Rev. B **103**, 144307 (2021).

[30] T. N. Ikeda and A. Polkovnikov, Fermi's golden rule for heating in strongly driven Floquet systems, Phys. Rev. B **104**, 134308 (2021).

[31] T. Prosen, Time evolution of a quantum many-body system: Transition from integrability to ergodicity in the thermodynamic limit, Phys. Rev. Lett. **80**, 1808 (1998).

[32] L. D'Alessio and A. Polkovnikov, Many-body energy localization transition in periodically driven systems, Ann. Phys. (Amsterdam) **333**, 19 (2013).

[33] D. V. Else, B. Bauer, and C. Nayak, Floquet time crystals, Phys. Rev. Lett. **117**, 090402 (2016).

[34] N. Y. Yao, A. C. Potter, I. D. Potirniche, and A. Vishwanath, Discrete time crystals: Rigidity, criticality, and realizations, Phys. Rev. Lett. **118**, 030401 (2017).

[35] M. Heyl, P. Hauke, and P. Zoller, Quantum localization bounds Trotter errors in digital quantum simulation, Sci. Adv. **5**, eaau8342 (2019).

[36] M. Medenjak, B. Buča, and D. Jaksch, Isolated Heisenberg magnet as a quantum time crystal, Phys. Rev. B **102**, 041117(R) (2020).

[37] A. Haldar, D. Sen, R. Moessner, and A. Das, Dynamical freezing and scar points in strongly driven Floquet matter: Resonance vs emergent conservation laws, Phys. Rev. X **11**, 021008 (2021).
[38] P. Emonts and I. Kukuljan, Reduced density matrix and entanglement of interacting quantum field theories with Hamiltonian truncation, Phys. Rev. Res. **4**, 033039 (2022).
[39] A. Rajak, R. Citro, and E. G. D. Torre, Stability and prethermalization in chains of classical kicked rotors, J. Phys. A **51**, 465001 (2018).
[40] O. Howell, P. Weinberg, D. Sels, A. Polkovnikov, and M. Bukov, Asymptotic prethermalization in periodically driven classical spin chains, Phys. Rev. Lett. **122**, 010602 (2019).
[41] T. Prosen, Chaos and complexity of quantum motion, J. Phys. A **40**, 7881 (2007).
[42] A. Haldar, R. Moessner, and A. Das, Onset of Floquet thermalization, Phys. Rev. B **97**, 245122 (2018).
[43] L. M. Sieberer, T. Olsacher, A. Elben, M. Heyl, P. Hauke, F. Haake, and P. Zoller, Digital quantum simulation, trotter errors, and quantum chaos of the kicked top, npj Quantum Inf. **5**, 78 (2019).
[44] C. Kargi, J. P. Dehollain, L. M. Sieberer, F. Henriques, T. Olsacher, P. Hauke, M. Heyl, P. Zoller, and N. K. Langford, Quantum chaos and universal trotterisation behaviours in digital quantum simulations, arXiv:2110.11113.
[45] E. Vernier, B. Bertini, G. Giudici, and L. Piroli, Integrable digital quantum simulation: Generalized Gibbs ensembles and trotter transitions, Phys. Rev. Lett. **130**, 260401 (2023).
[46] N. O'Dea, F. Burnell, A. Chandran, and V. Khemani, Prethermal stability of eigenstates under high frequency Floquet driving, Phys. Rev. Lett. **132**, 100401 (2024).
[47] Y. Suzuki, Y. Kawase, Y. Masumura, Y. Hiraga, M. Nakadai, J. Chen, K. M. Nakanishi, K. Mitarai, R. Imai, S. Tamiya, T. Yamamoto, T. Yan, T. Kawakubo, Y. O. Nakagawa, Y. Ibe, Y. Zhang, H. Yamashita, H. Yoshimura, A. Hayashi, and K. Fujii, Qulacs: A fast and versatile quantum circuit simulator for research purpose, Quantum **5**, 559 (2021).
[48] S. Blanes, F. Casas, J. A. Oteo, and J. Ros, The Magnus expansion and some of its applications, Phys. Rep. **470**, 151 (2009).
[49] See Supplemental Material at http://link.aps.org/supplemental/10.1103/PhysRevLett.133.030401 for additional data and arguments, which includes Refs. [50–57].
[50] A. Messiah, *Quantum Mechanics*, Dover Books on Physics (Dover Publications, Mineola, NY, 2014).
[51] D. W. Hone, R. Ketzmerick, and W. Kohn, Time-dependent Floquet theory and absence of an adiabatic limit, Phys. Rev. A **56**, 4045 (1997).
[52] D. Sels and A. Polkovnikov, Dynamical obstruction to localization in a disordered spin chain, Phys. Rev. E **104**, 054105 (2021).
[53] P. J. D. Crowley and A. Chandran, A constructive theory of the numerically accessible many-body localized to thermal crossover, SciPost Phys. **12**, 201 (2022).
[54] A. Morningstar, L. Colmenarez, V. Khemani, D. J. Luitz, and D. A. Huse, Avalanches and many-body resonances in many-body localized systems, Phys. Rev. B **105**, 174205 (2022).
[55] R. G. Pereira, S. R. White, and I. Affleck, Spectral function of spinless fermions on a one-dimensional lattice, Phys. Rev. B **79**, 165113 (2009).
[56] D. E. Parker, X. Cao, A. Avdoshkin, T. Scaffidi, and E. Altman, A universal operator growth hypothesis, Phys. Rev. X **9**, 041017 (2019).
[57] E. W. Weisstein, Jacobi Theta Functions. From MathWorld–A Wolfram Web Resource, https://mathworld.wolfram.com/JacobiThetaFunctions.html.
[58] K. Mallayya and M. Rigol, Heating rates in periodically driven strongly interacting quantum many-body systems, Phys. Rev. Lett. **123**, 240603 (2019).
[59] K. Mallayya, M. Rigol, and W. De Roeck, Prethermalization and thermalization in isolated quantum systems, Phys. Rev. X **9**, 021027 (2019).
[60] S. Sachdev, *Quantum Phase Transitions*, 2nd ed. (Cambridge University Press, Cambridge, England, 2011).
[61] M. Srednicki, The approach to thermal equilibrium in quantized chaotic systems, J. Phys. A **32**, 1163 (1999).
[62] L. D'Alessio, Y. Kafri, A. Polkovnikov, and M. Rigol, From quantum chaos and eigenstate thermalization to statistical mechanics and thermodynamics, Adv. Phys. **65**, 239 (2016).
[63] B. Evrard, A. Pizzi, S. I. Mistakidis, and C. B. Dag, Quantum scars and regular eigenstates in a chaotic spinor condensate, Phys. Rev. Lett. **132**, 020401 (2024).
[64] H. Sambe, Steady states and quasienergies of a quantum-mechanical system in an oscillating field, Phys. Rev. A **7**, 2203 (1973).
[65] M. Kormos, M. Collura, G. Takács, and P. Calabrese, Real-time confinement following a quantum quench to a non-integrable model, Nat. Phys. **13**, 246 (2017).
[66] O. A. Castro-Alvaredo, M. Lencsés, I. M. Szécsényi, and J. Viti, Entanglement oscillations near a quantum critical point, Phys. Rev. Lett. **124**, 230601 (2020).
[67] O. A. Castro-Alvaredo and D. X. Horvath, Branch point twist field form factors in the sine-Gordon model I: Breather fusion and entanglement dynamics, SciPost Phys. **10**, 132 (2021).
[68] P. Weinberg and M. Bukov, QuSpin: A Python package for dynamics and exact diagonalisation of quantum many body systems part I: Spin chains, SciPost Phys. **2**, 3 (2017).
[69] P. Weinberg and M. Bukov, QuSpin: A Python package for dynamics and exact diagonalisation of quantum many body systems. Part II: Bosons, fermions and higher spins, SciPost Phys. **7**, 20 (2019).